Reliability Engineering and System Safety 241 (2024) 109680

Contents lists available at ScienceDirect

Reliability Engineering and System Safety

journal homepage: www.elsevier.com/locate/ress

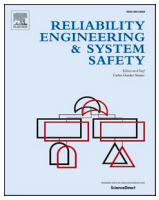

Consecutively connected systems with unreliable resource generators and storages

Gregory Levitin [a,b], Liudong Xing [c], Yuanshun Dai [a,*]

[a] School of Computing and Artificial Intelligence, Southwest Jiaotong University, China
[b] NOGA- Israel Independent System Operator, Israel
[c] University of Massachusetts, Dartmouth, MA 02747, United States

ARTICLE INFO

Keywords:
Linear consecutively connected system
Resource generation
Resource storage
Availability
Connectivity
Wireless sensor network

ABSTRACT

Motivated by real-world applications like wireless sensor networks powered by photovoltaic sources, this paper models a linear consecutively connected system whose nodes form a linear sequence. To provide the connectivity between the first (source) and last (destination) nodes, each non-destination node hosts a connecting element characterized by a different connection range and time-to-failure distribution. To supply resource needed for the connecting element's operation, each node also contains a resource generating subsystem and a storage, which is used for saving surplus resource when productivity of the resource generator exceeds the connecting element's demand and can also supply resource to the connecting element when the resource generator fails or its productivity becomes insufficient to meet the demand. A numerical algorithm is first put forward to evaluate the instantaneous availability of an individual connecting element. A universal generating function-based approach is further proposed to evaluate the instantaneous connectivity of the considered system with unreliable resource generators and storages. The optimal storage allocation problem and impacts of several parameters on the system connectivity and optimal solutions are investigated through a detailed case study of a wireless sensor network with four types of storages, characterized by different time-to-failure distributions, initial and maximum capacities, and maximum uploading and downloading rates.

1. Introduction

Many real-world systems (e.g., linear wireless sensor networks, radio communication systems, pipeline transportation systems, and production lines [1–4]) can be modeled as linear consecutively connected systems (LCCSs), where system nodes form a linear and ordered sequence and each node hosts a connection element (CE) to provide a connection between the host node and its subsequent nodes along the sequence [5]. The CEs allocated to different nodes may have different connection ranges and different time-to-failure distributions; they work together to provide the connectivity between the source (first) and destination (last) nodes [6,7]. Due to the heterogeneity of CEs, different CEs allocation schemes may lead to significantly different connectivity performance of LCCSs. Thus, it is relevant and pivotal to solve the optimal CE allocation problem to maximize the LCCS performance [8,9].

Considerable research efforts have been devoted to addressing the optimal CE allocation problem for LCCSs with different features. For example, the allocation problem was solved for LCCSs subject to multiple and consecutive phases of operations where different source and destination nodes are engaged in different phases [10]. In [11], the problem was solved for multi-phase LCCSs subject to common-cause failures where a shared root cause may incur simultaneous malfunctions of multiple CEs. In [12] and [13], extensions were respectively made to the traditional single-phase and multi-phase LCCS models by allowing a certain number of single-node gaps (disconnected nodes) for the system functionality. In [14], the LCCS model that can tolerate a certain size of consecutive gaps was considered. In [15,16], the LCCS model tolerating a combination of single-node gaps and consecutive gaps were optimized. In [17], the allocation problem was solved for LCCSs with warm standby redundancy. In [18], the preventive replacement and corrective maintenance with constant average repair time and minimal repair policy of CEs were modeled. In [11,19], random repair time and general repair policy (covering the minimal repair, perfect repair, and imperfect repair) of CEs were modeled.

To the best of our knowledge, none of the existing LCCS models addressed the resource generation and storage units that supply the resource (e.g., power) necessary for the CE's function. In particular, the

* Corresponding author.
E-mail address: 1125105129@qq.com (Y. Dai).

https://doi.org/10.1016/j.ress.2023.109680
Received 6 July 2023; Received in revised form 20 September 2023; Accepted 21 September 2023
Available online 23 September 2023

Acronyms

RGS	resource generation subsystem
CE	connecting element
LCCS	linear consecutively connected system
ILC	instantaneous LCCS connectivity
ELC	expected LCCS connectivity
cdf	cumulative distribution function
pdf	probability density function

Notations

M	number of CEs in LCCS
T	mission time
c_m	capacity of storage m
u_m	maximum uploading rate of storage m
w_m	maximum downloading rate of storage m
d_m	resource demand of CE m
l_m	maximum connection range of CE m
$g_m(t)$	productivity of RGS m at time t
$Q_m(t)$	probability that demand of CE m is supplied at time t
$a_m(t)$	instantaneous availability of individual CE m
$L_m(t)$	random connection range of CE m at time t
$A(t)$	instantaneous availability of LCCS
$E(T)$	ELC during mission time T
$x_m(t)$	amount of resource in storage m at time t given that RGS and storage are available
$x_m(0)$	amount of resource in storage m at the beginning of mission
$F_m(t)$	*cdf* of time-to-failure distribution for CE m
$Y_m(t)$	*cdf* of time-to-failure distribution of resource storage of CE m
$v_m(t), V_m(t)$	*pdf, cdf* of time-to-failure distribution of RGS of CE m
$\Pr(X)$	probability of event X
$1(Z)$	indicator function: 1(TRUE)=1, 1(FALSE)=0

storage is used to store surplus resource, which may subsequently be utilized to supply the system demand when the resource generation unit fails, or its productivity is insufficient. A set of diverse methods have been suggested for incorporating the storage in the system reliability analysis, including, for example, the universal generating functions-based method for multi-phase performance sharing systems [20], the semi-Markov processes-based method for multi-production line chemical process plants [21], the discrete-event simulation method for multi-state industrial processes [22], the probabilistic modeling method for warm standby systems [23], the multivalued decision diagrams-based methods for phased-mission systems [24] and demand-based standby systems [25], the numerical methods for multi-state systems with mission aborting [26], and non-repairable systems with multiple storage units used in parallel [27] or consecutively [28]. However, none of those methods considering storage are directly applicable to modeling and analyzing LCCSs.

This work contributes by pioneering the modeling of binary-state LCCSs with unreliable resource generation and storages. Specifically, to supply resource needed for the operation of each CE, each node of the LCCS contains a resource generating subsystem (RGS), which has certain productivity when operating. Each RGS may be equipped with a resource storage characterized by maximum capacity as well as maximum uploading and downloading rates. The storage can save the surplus resource when the RGS's productivity exceeds the CE's demand and can also supply resource to the CE when the RGS fails or its productivity becomes insufficient to meet the CE's demand. We propose a numerical algorithm to evaluate the instantaneous availability of an individual CE. We further use a universal generating function-based approach to evaluate the instantaneous connectivity of the considered LCCS, based on which the expected LCCS connectivity (ELC) can be computed. We formulate and solve the optimal storage allocation problem maximizing the ELC and examine impacts of several model parameters through a detailed case study of a wireless sensor network LCCS.

The remainder of the paper is structured as follows. Section 2 depicts the LCCS model considered in this work and definitions of the instantaneous LCCS connectivity and ELC. Section 3 suggests the numerical algorithm that evaluates the instantaneous availability of an individual CE and investigates the effects of initial amount of resource and maximal downloading rate of the storage through an example. Section 4 describes the universal generating function-based method to evaluate the instantaneous LCCS connectivity. Section 5 presents the detailed case study and examines the influences of several model parameters. Section 6 provides conclusions and several further research topics.

2. System model

The binary-state LCCS consists of $M+1$ consecutive nodes (locations). CEs are located at each of the first M nodes to provide a connection between the first (source) node and the $M+1$-th (sink) node. Each CE located at node m ($1 \le m \le M$) is characterized by a specific connection range l_m, and time-to-failure cumulative distribution function (*cdf*) $F_m(t)$. Thus, the most remote node that can be reached by this CE at time t is $m+L_m(t)$, where $\Pr(L_m(t) = l_m) = a_m(t)$, $\Pr(L_m(t) = 0) = 1 - a_m(t)$ and $a_m(t)$ is the instantaneous availability of CE m at time t (evaluated in Section 3). The most remote node that can be reached by the group of CEs located at the first k nodes (i.e., nodes 1, 2,…, k) at time t is

$$H_k(t) = \min\left\{M+1, \max_{1\le m\le k}\{m + L_m(t)\}\right\}. \quad (1)$$

In case of $H_k(t) < k+1$ for any k ($1 \le k \le M$), node $k+1$ is disconnected from all the preceding nodes, and thus the source and sink nodes cannot be connected. Therefore, the connectivity condition of the considered LCCS at time t is

$$\varphi(L_1(t), \ldots, L_M(t)) = \prod_{k=1}^{M} 1(H_k(t) > k), \quad (2)$$

which returns 1 if the LCCS is connected and 0 otherwise.

The considered LCCS can be found in many applications. For example, a pipe flow transmission system has pumps that are distributed among certain locations along the pipeline. The pump (i.e., CE) residing at a location m provides necessary pressure to transfer the flow to the next $L_m(t)$ locations [12]. The distance between the consecutive locations can vary depending on geographical and environmental conditions, which affects the connection ranges and repair times of different pumps. The pipeline fails if the flow transmission between the source and sink locations cannot be maintained.

Another example of LCCS applications is a radio communication system, which consists of a set of radio relay stations (nodes) with a transmitter allocated at station 1 and a receiver allocated at the last station $M+1$. To provide signal propagation from the transmitter to the receiver, some re-transmitters (i.e., CEs) are deployed. Specifically, each station m ($2 \le m \le M$) can have a re-transmitter relaying signals that reach the next $L_m(t)$ stations. The connection range $L_m(t)$ depends on the amplifier's power of re-transmitter m and on the distance between node m and its subsequent nodes. Fig. 1 presents an example of a radio communication system with $M = 6$, L_1=L_3=L_5=2, L_2=L_6=1 and L_4=3 when it provides connection between the transmitter and the receiver

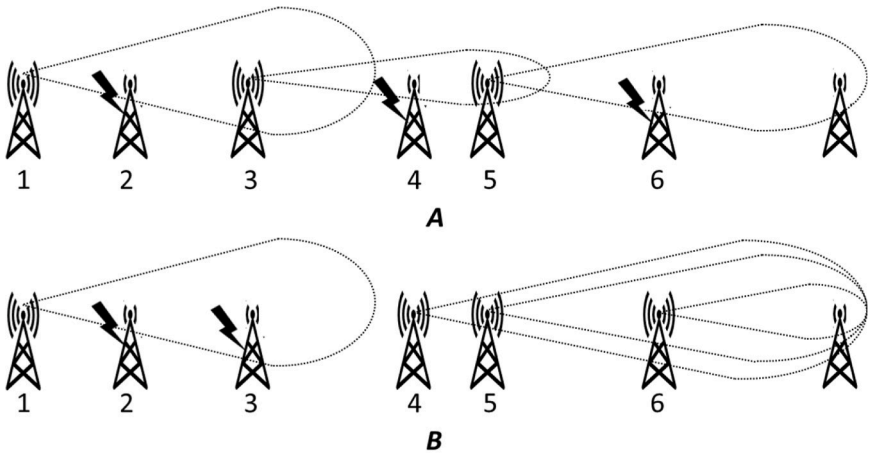

Fig. 1. An example of a radio communication LCCS in the connected state (A) and disconnected state (B).

despite the failure of stations 2 and 4 (scenario (A)), and when it fails to provide such connection because of the failure of stations 2 and 3 (scenario (B)).

An example of a wireless sensor network is also presented in Section 5.

The instantaneous LCCS connectivity (ILC) at a particular time instant t can be defined as $A(t)=\Pr(\varphi(L_1(t), \ldots, L_M(t))=1)$. Usually, technical systems are planned to operate during a specific time horizon, after which their elements are replaced or repaired and/or structure is changed (due to changes in technology, conditions of functioning and/or system mission). Thus, the availability analysis beyond the planned horizon has no sense and the LCCS behavior is modeled within a time horizon T. The expected LCCS connectivity (ELC) during the mission time T can thus be obtained as

$$E(T) = \frac{1}{T}\int_0^T A(t)dt \tag{3}$$

Each CE m consumes per unit time amount or resource (demand) d_m needed for its operation. Therefore, each node contains a RGS aimed at supplying the resource demand. The per unit time amount of resource generated by the RGS m (productivity) $g_m(t)$ varies with time. Besides, the RGS can fail. If the demand d_m is not satisfied, the CE m cannot provide connection to the next nodes and $L_m(t) = 0$. The *cdf* of time-to-failure of RGS m is $V_m(t)$.

To enhance the resource supply reliability by supplying the CE when the generation rate of the RGS is insufficient or when the RGS fails, RGS m can be equipped with a resource storage having a given capacity c_m and maximum uploading and downloading rates of u_m and w_m, respectively (see Fig. 2). When the RGS productivity exceeds the demand ($g_m(t) > d_m$) and the storage is available and not fully loaded, the surplus resource is uploaded to the storage with rate not exceeding u_m. When the RGS productivity is insufficient ($g_m(t) < d_m$), the storage is available and not empty and the resource deficiency does not exceed the maximum storage downloading rate (i.e., $d_m - g_m(t) < w_m$), the storage is downloaded with rate $d_m - g_m(t)$ and the CE demand is satisfied. When the RGS productivity is insufficient, the storage is available and not empty, but the resource deficiency exceeds the maximum storage downloading rate, the CE demand cannot be satisfied anyway and if the storage is not fully loaded, it is uploaded from the RGS with rate $min(u_m, g_m(t))$.

When both RGS and resource storage of CE m are available at time t, the change in the amount of the resource accumulated in the storage during time interval $[t,t+dt)$, where dt is infinitesimal is

$$\begin{aligned}\delta x_m(t) = {} & 1(g_m(t) > d_m)min(u_m, (g_m(t) - d_m))dt \\ & +1(d_m - g_m(t) > w_m)min(u_m, g_m(t))dt - 1(0 < d_m - g_m(t) \le w_m)(d_m - g_m(t))dt,\end{aligned} \tag{4}$$

where the first term corresponds to the case where the RGS supplies both CE and storage, the second term corresponds to the case where the RGS and the storage cannot satisfy the demand and the RGS supplies the storage, and the third term corresponds to the case where both RGS and storage supply the demand.

The total amount of the resource accumulated in the storage by time t

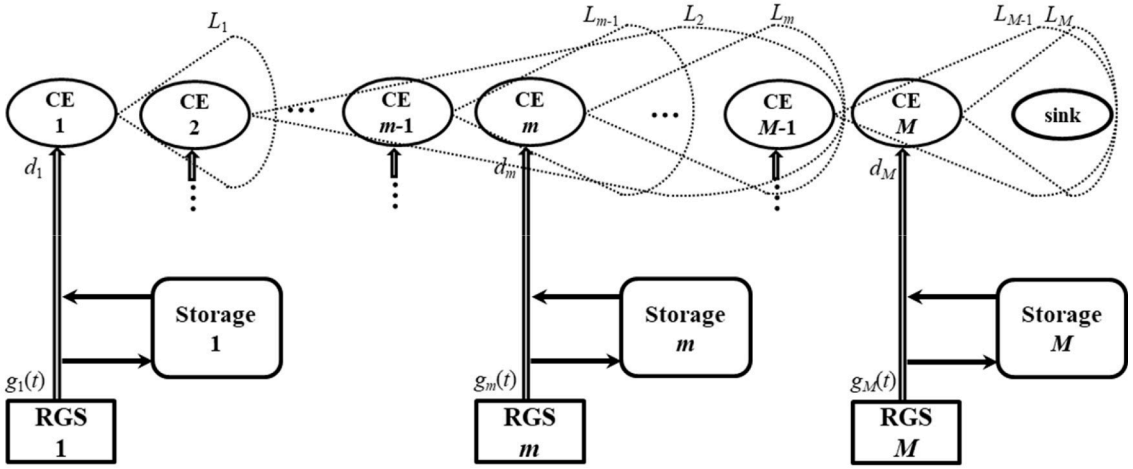

Fig. 2. Structure of the LCCS with RGSs and storages.

can be obtained iteratively for $t=dt,2dt,\ldots,T$

$$x_m(t) = min(c_m, max(0, x_m(t-dt) + \delta x_m(t))), \quad (5)$$

where $x_m(0)$ is the initial amount of resource in the storage at the beginning of the mission.

Fig. 3 presents an example of the CE performance when both RGS and storage are available and $w_m<d_m$. It can be seen that the CE is unable to provide connection to other nodes when the resource deficiency exceeds the maximum storage downloading rate or when the storage is empty and cannot compensate any resource deficiency.

3. Instantaneous availability of individual CEs

The demand of CE m can be satisfied at time t in the following three cases:

1. RGS m is available at time t and its productivity is not lower than the demand d_m: $g_m(t) \geq d_m$;
2. Both RGS m and storage m are available at time t, $0<d_m-g_m(t)\leq w_m$ and $x_m(t)>0$, i.e., the resource deficiency is compensated from the storage;
3. RGS m fails at time $\tau<t$, but the storage still operates at time t, the demand d_m does not exceed the maximum storage downloading rate w_m and the resource in the storage is not depleted till time t, i.e., $x_m(t)=x_m(\tau)-(t-\tau)d_m\geq 0$.

The probability that the RGS m fails in time interval $[\tau,\tau+d\tau)$, where $d\tau$ is infinitesimal, is $v_m(\tau)d\tau$. Thus, we can obtain the probability that the resource m is supplied at time t (instantaneous availability of CE m supply system) as

$$\begin{aligned} Q_m(t) &= 1(g_m(t) \geq d_m)(1 - V_m(t)) \\ &+1(0 < d_m - g_m(t) \leq w_m)1(x_m(t) > 0)(1 - V_m(t))(1 - Y_m(t)) \\ &+1(d_m \leq w_m)(1 - Y_m(t)) \int_0^t 1(x_m(\tau) > (t-\tau)d_m)v_m(\tau)d\tau \end{aligned} \quad (6)$$

where the three terms correspond to the three cases above.

When the resource supply system of CE m does not contain storage ($c_m = u_m = w_m = 0$), the resource m can be supplied at time t only if the corresponding RGS is available and $g_m(t) \geq d_m$. In this case

$$Q_m(t) = 1(g_m(t) \geq d_m)(1 - V_m(t)).$$

The instantaneous availability of CE m at time t can be obtained as

$$a_m(t) = (1 - F_m(t))Q_m(t). \quad (7)$$

3.1. Numerical evaluation algorithm

To realize the derivations presented above in a numerical procedure, we obtain the amount of resource in the storage recursively according to (4) and (5). For each time interval $[t,t+dt)$, we obtain the values of $Q_m(t)$ for the cases where the RGS is available using the first two terms of (6). Instead of the backward equation for the third term of (6), we use a forward procedure that updates the values of $Q_m(\tau+t)$ for any realization t of the RGS failure time and any realization τ of the storage downloading time after the RGS failure. The pseudo-code of the numerical procedure for evaluating the instantaneous CE availability is as follows.

```
1   For m = 1,...,M :
2       x = x_m(0);
3       For t = 0, dt, ...,T :  q_m(t) = 0;
4       For t = 0, dt, ...,T :
5           δ = Δ = g_m(t) − d_m; //Δ − surplus resource generated by RGS
6           If Δ > u_m then δ = u_m; //δ – storage uploading pace
7           If Δ < −w_m then δ = min(u_m,g_m(t)); //demand cannot be met
8           x = x + δdt;
9           If x > c_m then x = c_m;
10          If x < 0 then x = 0; //amount of resource in the storage
11          If Δ ≥ 0 then q_m(t) = q_m(t) + 1 − V_m(t); //RGS supplies the demand
12          If −w_m ≤ Δ < 0 AND x>0 then q_m(t) = q_m(t) + (1 − V_m(t))(1 −
            Y_m(t));
13          If d_m ≤ w_m then For τ = 0, dt, ...,min(T − t, x/d_m) :
14              q_m(t + τ) = q_m(t + τ) + (V_m(t + dt) − V_m(t))Y_m(t + τ);
15      a_m(t) = (1 − F_m(t))q_m(t);
```

Steps 5 – 7 of the pseudo-code determine the variation of amount of the resource accumulated in the storage during time interval $[t,t+dt)$ according to (4). Steps 8 – 10 determine the amount of resource in the

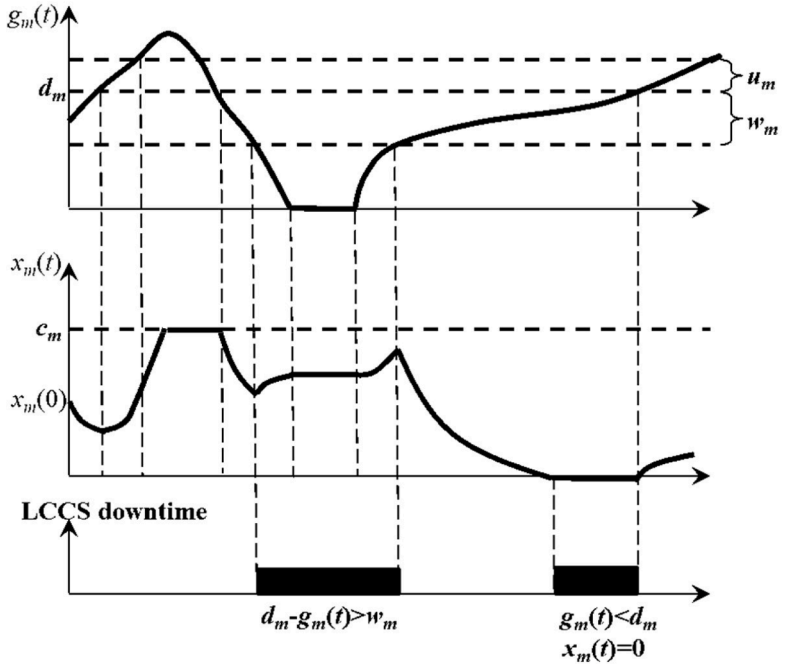

Fig. 3. Example of CE performance when all its components are available.

storage at time t. Step 11 updates the resource availability at time t in the case where RGS operates and its productivity $g_m(t)$ exceeds the demand d_m. Step 12 updates the resource availability at time t in the case where both RGS and storage operate and insufficient RGS productivity $g_m(t)$ is compensated from the storage. Steps 13 and 14 update the resource availability at time $t+\tau$ when the RGS fails at time t and the demand is supplied from the storage.

As it can be seen from the pseudo-code, the computational complexity of the numerical procedure is $O(M\,dt^{-2})$.

3.2. Illustrative example

Consider a CE with demand $d = 0.09$ and time-to-failure *cdf* $F(t) = 1 - \exp(-t/180)$, which is supplied from a RGS having time-to-failure *cdf* $V(t) = 1 - \exp(-(t/220)^{1.1})$. The RGS provides time dependent per unit time amount of resource $g(t) = 0.1\max(0, 0.2 + \sin(0.26t + 0.2))$. The RGS is equipped with a storage with capacity $c = 12$, time-to-failure distribution *cdf* $Y(t) = 1 - \exp(-(t/80)^{1.1})$, maximum uploading and downloading paces $u = w = 0.1$.

Fig. 4 presents the difference between the produced resource and demand $g(t)$-d, dynamic amount of resource in the storage $x(t)$ when no failures occur and instantaneous availability of the CE $a(t)$ for different levels of initial amount of resource in the storage $x(0)$. It can be seen that the instantaneous availability sharply increases when the RGS has enough resource to supply the demand without using the storage. The amount of resource in the storage increases when the resource generation rate exceeds the CE's demand and decreases when the resource generation rate is insufficient and the deficiency is compensated from the storage. When the storage is emptied, the demand cannot be met if the resource generation rate is lower than the demand d and the instantaneous availability is zeroed. The increase in the initial amount of resource in the storage allows the storage to supply the resource to the CE for a longer time before the storage is empty. This causes an increase in the periods when the CE is available. For example, when $x(0)$=0, the storage cannot supply the CE at the beginning of the mission and the CE remains unavailable until the RGS productivity exceeds the demand. When $x(0)$=2, the storage is emptied for the first time at $t = 44.5$ causing the CE's unavailability. Observe that when $x(0)\leq 2$, the CE remains unavailable during some periods of the mission even when the storage, the RGS and the CE do not fail. When $x(0)$=5, the storage is never emptied during the mission and the CE has enough resource to operate without interruptions if the storage, the RGS and the CE are available. The expected CE availability during the mission having a duration of $T = 72$ h is 0.23 for $x(0)$=0, 0.45 for $x(0)$=2, and 0.53 for $x(0)$=5.

Fig. 5 presents the difference between the produced resource and demand $g(t)$-d, dynamic amount of resource in the storage $x(t)$ when no failures occur and instantaneous availability of the CE $a(t)$ for different values of maximal downloading rate of the storage w when $x(0)$=2. When w is low ($w = 0.02$), the storage cannot compensate the resource deficiency when d-$g(t)>w$ and is uploaded for a longer time (when the demand cannot be met anyway). In this case, the amount of resource in the storage x increases whereas the instantaneous availability of the CE remains zero for a long time. When w increases ($w = 0.08$) the periods when d-$g(t)>w$ become shorter and the storage contributes to supplying the resource to the CE during longer periods. The amount of resource in the storage x decreases. When w exceeds the demand ($w = 0.1>d = 0.09$), the storage can supply the stored resource to the CE any time when the RGS productivity is insufficient. Thus, the instantaneous CE availability is not zeroed until the storage emptying at time $t = 44.6$. Though the storage is emptied faster than in the cases of lower w, its efficiency in maintaining the CE available increases. The expected CE availability during the mission with a duration of $T = 72$ h is 0.21 for $w = 0.02$, 0.31 for $w = 0.08$, and 0.45 for $w = 1$.

4. ILC evaluation using the universal generating function method

Following a brief background on the universal generating function, this section presents the method to obtain ILC $A(t)$=Pr($\varphi(L_1(t), \ldots, L_M(t))$=1) based on $a_m(t)$ for $1 \leq m \leq M$ derived in Section 3.

Consider a discrete random variable $B(t)$ that can take K possible values, and $q_k(t)$=Pr{$B(t)$=b_k}. The universal generating function representing its *pmf* is $u_B(z,t) = \sum_{k=1}^{K} q_k(t) z^{b_k}$ [6]. Similarly, $C(t)$ is another random variable with I possible values and universal generating function $u_C(z,t) = \sum_{i=1}^{I} p_i(t) z^{c_i}$. Assume that $B(t)$ and $C(t)$ are statistically independent. Then the universal generating function denoting the distribution of function $\gamma(B(t),C(t))$ can be obtained using the composition operator defined in (8).

$$u_B(z,t) \underset{\gamma}{\otimes} u_C(z,t) = \sum_{k=1}^{K} q_k(t) z^{b_k} \underset{\gamma}{\otimes} \sum_{i=1}^{I} p_i(t) z^{c_i} = \sum_{k=1}^{K} \sum_{i=1}^{I} q_k(t) p_i(t) z^{\gamma(b_k,c_i)} \quad (8)$$

where $q_k(t)p_i(t)$ gives Pr{($B(t)$=b_k)∩($C(t)$=c_i)}.

The evaluation of ILC involves two universal generating functions

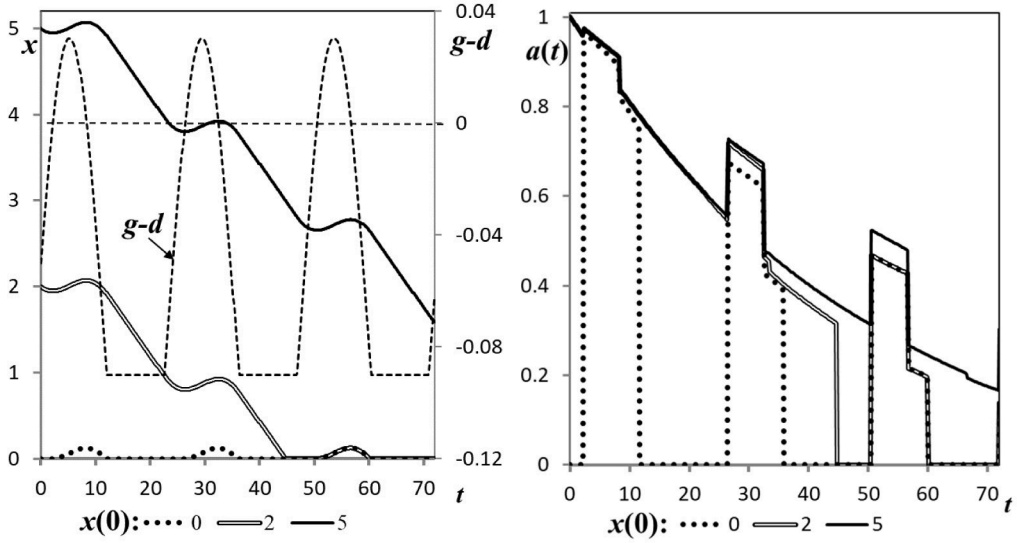

Fig. 4. Difference between RGS productivity and demand $g(t)$-d, dynamic amount of resource in the storage $x(t)$ and instantaneous availability of the CE $a(t)$ for different levels of initial amount of resource in the storage $x(0)$.

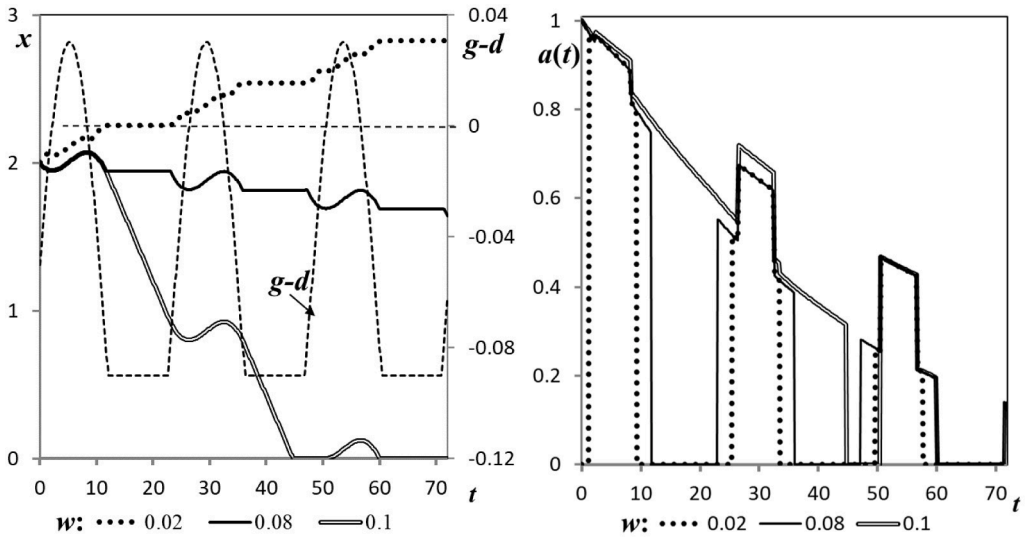

Fig. 5. Difference between RGS productivity and demand $g(t)$-d, dynamic amount of resource in the storage $x(t)$ and instantaneous availability of the CE $a(t)$ for different values of maximal downloading rate of the storage w when $x(0)$=2.

$$u_m(z,t) = a_m(t)z^{l_m} + (1 - a_m(t))z^0;$$
$$U_k(z,t) = \sum_{h=k}^{M+1} \pi_{k,h}(t)z^h, \text{ where} \pi_{k,h}(t) = Pr\{H_k(t) = h\} \text{ and } U_0(z,t) \equiv z^1, \tag{9}$$

which respectively represent the distribution of $L_m(t)$ and distribution of $H_k(t)$ defined in (1). Function (1) can be represented recursively as

$$H_k(t) = \min\{M+1, \max\{H_{k-1,h}, k + L_k(t)\}\}. \tag{10}$$

Thus, the universal generating function $U_k(z,t)$ for $k = 1,\ldots,M$ can be determined using the following recursive procedure

$$U_k(z,t) = U_{k-1}(z,t) \underset{minmax}{\otimes} u_k(z,t) = \sum_{h=k}^{M+1} \pi_{k,h}(t)z^h$$
$$= \sum_{h=k-1}^{M+1} \left(\pi_{k-1,h}(t)a_k(t)z^{\min\{M+1,\max\{h,k+l_k\}\}} + \pi_{k-1,h}(t)(1 - a_k(t))z^h\right). \tag{11}$$

Notice that the term with $L_k(t)$=k corresponds to disconnection of node k from further nodes and makes no contribution to the LCCS connectivity. This term should be removed from the function $U_k(z,t)$, which is made by the following operator

$$\theta(U_k(z,t)) = \theta\left(\sum_{h=k}^{M+1} \pi_{k,h}(t)z^h\right) = \sum_{h=k+1}^{M+1} \pi_{k,h}(t)z^h. \tag{12}$$

Applying $U_k(z,t) = \theta\left(U_{k-1}(z,t) \underset{minmax}{\otimes} u_k(z,t)\right)$ recursively, we can obtain the single-term function of $U_M(z,t) = \pi_{M,M+1}(t)z^{M+1}$, where $\pi_{M,M+1}(t)$ is the probability that nodes 1 and $M+1$ are connected at time t (i.e., ILC).

The following summarizes the universal generating function-based algorithm for determining ILC $A(t)$ for a given allocation of CEs and configuration of the resource supply subsystems.

1. Determine the instantaneous availability $a_m(t)$ of CEs in each node m for $m = 1,\ldots, M$ and for $t = 0, dt, \ldots, T$ using the algorithm presented in Section 3.
2. Define $U_0(z) \equiv z^1$ and $u_m(z,t) = a_m(t)z^{l_m} + (1 - a_m)z^0$ for $m = 1, \ldots, M$.
3. Apply $U_k(z,t) = \theta\left(U_{k-1}(z,t) \underset{minmax}{\otimes} u_k(z,t)\right)$ recursively for $k = 1, \ldots, M$.
4. Determine ILC $A(t)$ as coefficient $\pi_{M,M+1}$ of $U_M(z,t)$.

5. Case study

Consider a wireless sensor network used in applications such as environmental monitoring, infrastructure monitoring, smart homes or

Table 1
Parameters of sensors and their power sources.

m	η_m	β_m	l_m	d_m (kW)	ρ_m	μ_m	λ_m (kW)	Battery type
1	1.2	880	4	0.20	1.0	600	0.75	2
2	1.0	750	3	0.09	1.1	510	0.12	1
3	1.0	970	3	0.12	1.0	700	0.18	1
4	1.2	320	2	0.08	1.3	350	0.48	–
5	1.0	480	5	0.20	1.0	600	0.24	3
6	1.4	900	4	0.08	1.2	580	0.48	–
7	1.0	320	2	0.10	1.5	440	0.18	4
8	1.1	760	3	0.10	1.3	920	0.24	1
9	1.2	500	1	0.08	1.3	750	0.18	–

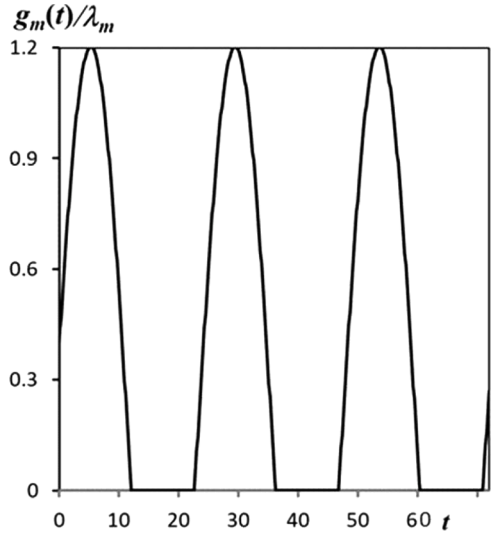

Fig. 6. Normalized power produced by photovoltaic power sources during the mission time.

Table 2
Parameters of batteries.

Type k	No of batteries	ξ_k	ϑ_k	c_k (kWh)	x_k (0) (kWh)	u_k (kW)	w_k (kW)
1	3	80	1.1	4	4	0.05	0.10
2	1	100	1.8	10	10	0.12	0.22
3	1	120	1.2	5	5	0.18	0.26
4	1	120	1.2	5	5	0.08	0.16

offices, smart agriculture, and battlefield surveillance [29–33]. The network consists of $M = 9$ sensor/actuator devices and must provide communications and sensing coverage through connections along a specific path of nodes. Depending on its transmission range, each device located at node m (when available) can provide a connection between node m and l_m next nodes along the path. Each device is equipped with photovoltaic power source. The generated power depends on the time of day and varies cyclically. To provide the power supply stability, the power accumulating batteries can be connected to each power source. In the case of the sensor device failure or the power loss, the node becomes disconnected from other nodes. The inter-maintenance period of the wireless sensor network is $T = 72$h

The reliability and power parameters of sensors, power sources and batteries are available from equipment manufacturers/providers. A wide range of the considered electronic equipment has time-to-failure obeying the Weibull distribution (see [34–37]). Specifically, the time-to-failure of the sensor device located at node m obeys the Weibull distribution with *cdf* $F_m(t) = 1 - \exp(-(t/\eta_m)^{\beta_m})$ [34,35]. The values of β_m and η_m as well as provided connection distance l_m and the power demand of each device d_m are presented in Table 1. Note that the connection ranges depend on specific conditions and can be determined experimentally.

The time-to-failure of the power source located at node m obeys the Weibull distribution [36] with *cdf* $V_m(t) = 1 - \exp(-(t/\rho_m)^{\mu_m})$. The values of ρ_m and μ_m are presented in Table 1. The varying power generated by photovoltaic source located at node m depends on its installed power and time of the day and can be approximated by the function

$$g_m(t) = \lambda_m \max(0, 0.2 + \sin(0.26t + 0.2))/1.1975, \tag{13}$$

where λ_m is the maximum generated power (see Fig. 6) with values presented in Table 1.

Six batteries of four different types are distributed among the nodes

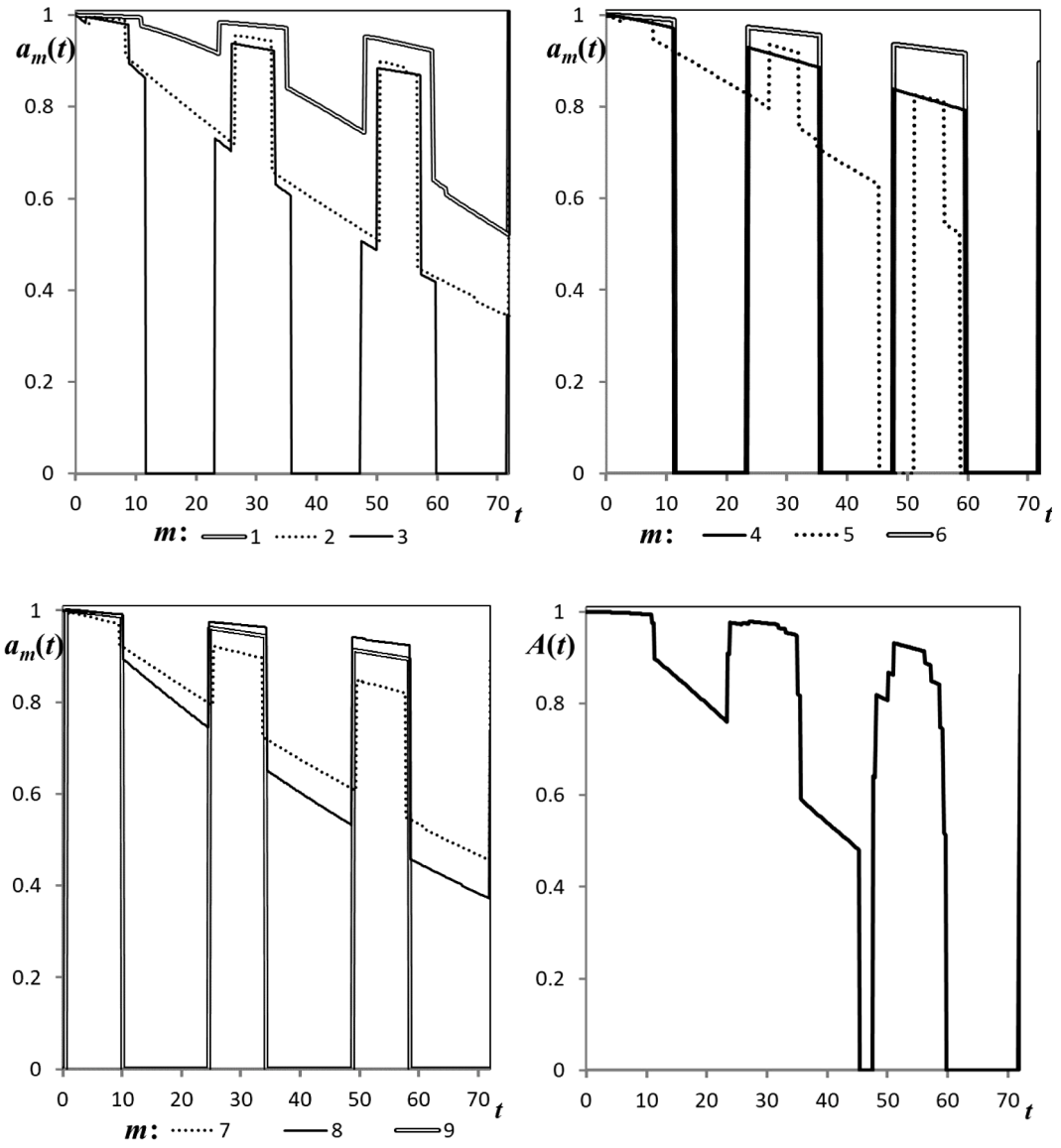

Fig. 7. Instantaneous availabilities of the individual CEs $a_m(t)$ and the ILC A(t) for batteries allocation presented in Table 1.

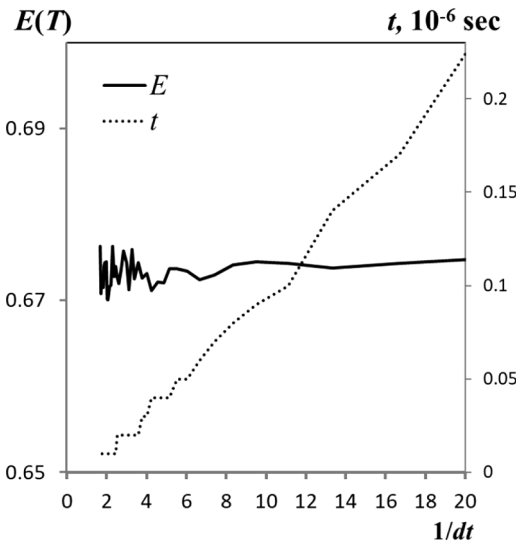

Fig. 8. ELC and running time as functions of the discretization parameter *dt*.

of the wireless sensor network. Table 1 presents types of the batteries located at each node (- corresponds to no battery). The time-to-failure distribution of battery of type k is Weibull [37] with the *cdf* taking the form $Y_k = 1 - \exp(-(t/\xi_k)^{\vartheta_k})$. The parameters of this distribution, the battery capacity c_k, the maximum charge and discharge power (u_k and w_k) and the initial charge level $x_k(0)$ are presented in Table 2. The instantaneous availabilities of the individual CEs $a_m(t)$ and the ILC A(t) are presented in Fig. 7. The ELC of the wireless sensor network during the inter-maintenance period $T = 72$ is $E(72)$=0.675.

5.1. Influence of the discretization factor dt on ELC evaluation accuracy

To evaluate the influence of the discretization factor *dt* on the ELC evaluation accuracy, we obtain the ELC E as a function of *dt*. Fig. 8 presents $E(T)$ and the running time of the C language realization of the numerical algorithm (Section 4) on 3.7 GHz PC as functions of the discretization factor *dt*. The obtained values of ELC quickly converge with a decrease in *dt*. The related discrepancy between $E(0.02)$ and $E(0.6)$ is 0.19% and between $E(0.02)$ and $E(0.1)$ is 0.1%. In further optimization examples, dt=0.05 is chosen.

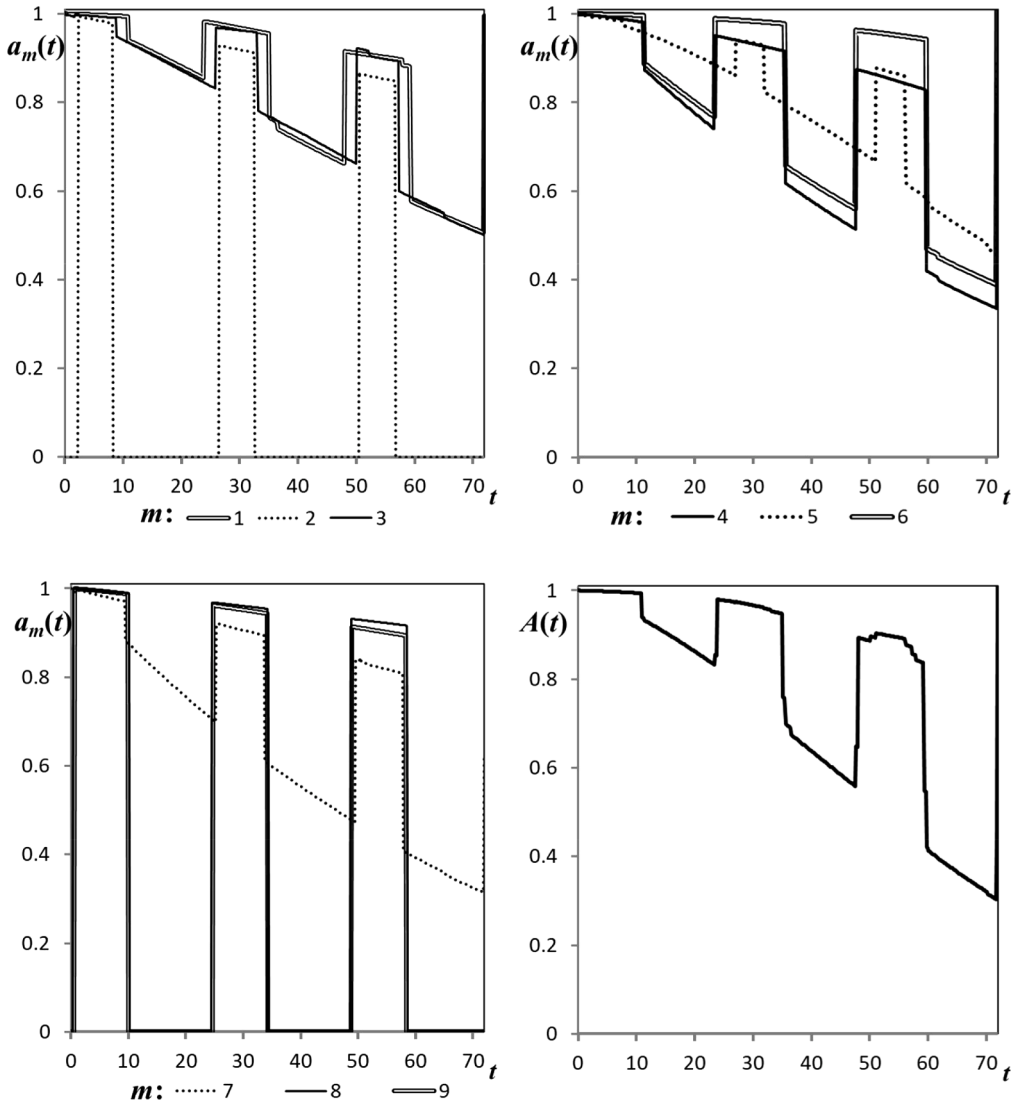

Fig. 9. Instantaneous availabilities of the individual CEs $a_m(t)$ and the ILC A(t) for the optimal batteries' allocation.

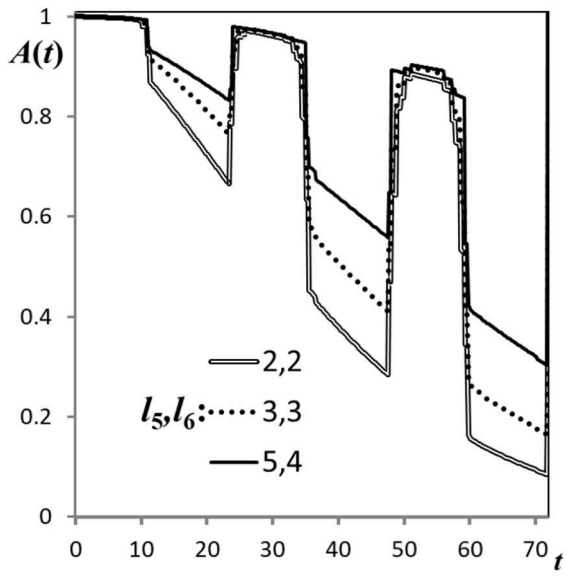

Fig. 10. ILC $A(t)$ for the optimal batteries' allocation when $l_5 = 5, l_6 = 4$; $l_5 = l_6 = 3$ and $l_5 = l_6 = 2$.

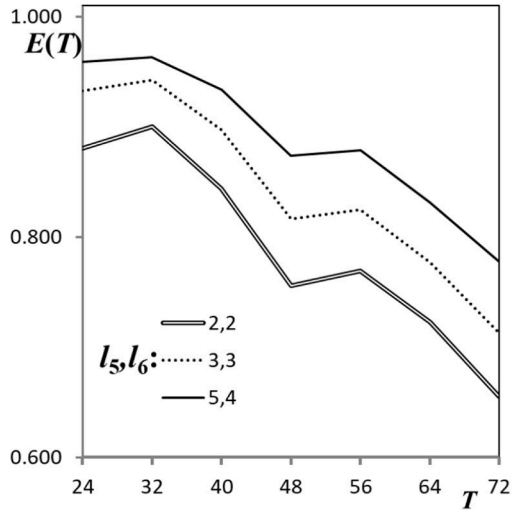

Fig. 11. ELC $E(T)$ for the optimal batteries' allocation as a function of the inter-maintenance time T.

5.2. Optimal batteries distribution problem and solution

If the batteries can be re-distributed among the nodes, the problem of the optimal batteries' distribution arises. Any distribution can be represented by vector $\boldsymbol{b}=\{b_1,\ldots,b_M\}$, where b_m is the type of the battery located in node m. The optimal distribution problem lies in finding the distribution maximizing the ELC:

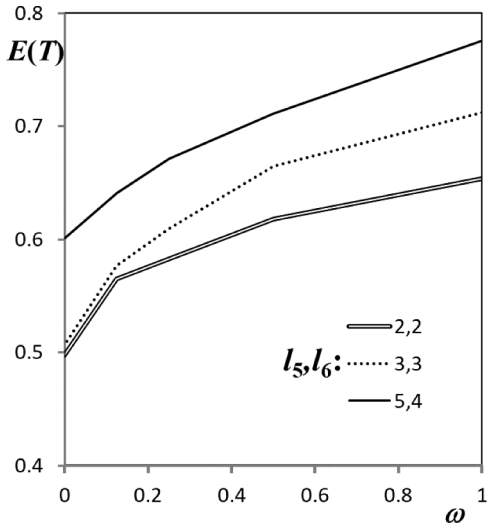

Fig. 12. ELC $E(T)$ for the optimal batteries' allocation as a function of the initial charge of the batteries.

$$\boldsymbol{b}=\arg\max_{\boldsymbol{b}} E(\boldsymbol{b},T),\ \text{subject to}\ \sum_{m=1}^{M} 1(b_m=k)=N_k\ \text{for}\ k=1,\cdots,K,$$

where N_k is the number of available batteries of type k and K is the number of different types of batteries.

For a large number of nodes and batteries, the problem can be solved using heuristics like genetic algorithm [38,39]. In the considered case where $M = 9$, $K = 4$ and $\sum_{k=1}^{K} N_k = 6$, a brute force enumeration is used for obtaining the optimal distribution.

Fig. 9 presents the instantaneous availabilities of the individual CEs $a_m(t)$ and the ILC $A(t)$ for the optimal batteries' allocation $\boldsymbol{b}$={3,-,4,1,2,1,1,-,-} providing the ELC $E(72)$=0.776, which is considerably greater than for the allocation presented in Table 1.

5.3. Influence of variation of system functioning conditions on the optimal solution

The suggested model allows analyzing the influence of variation of system functioning conditions on the optimal batteries distribution. For example, consider a situation where the signal transmission conditions in the area deploying sensors 5 and 6 deteriorate and the signal transmission ranges decrease such that $l_5 = l_6 = 3$. In this case, the optimal batteries allocation changes to $\boldsymbol{b}$={3,-,-,1,2,1,-,4,1}, which gives the ELC $E(72)$=0.712. The further decrease of the transmission ranges to $l_5 = l_6 = 2$ causes a change of the optimal batteries allocation to $\boldsymbol{b}$={3,-,-,-,2,1,1,4,1}, which gives the ELC $E(72)$=0.654. The ILC corresponding to these two cases and to the initial case of $l_5 = 5, l_6 = 4$ are presented in Fig. 10.

Table 3
Optimal batteries distribution for different system inter-maintenance times T and signal transmission ranges l_5, l_6.

	$l_5 = l_6 = 2$		$l_5 = l_6 = 3$		$l_5 = 5, l_6 = 4$	
T	b	$E(T)$	b	$E(T)$	b	$E(T)$
24	2,-,-,1,3,1,1,4,-	0.880	2,-,-,1,3,1,-,4,1	0.933	2,-,4,1,3,1,-,-,1	0.959
32	2,-,-,1,3,1,1,4,-	0.900	2,-,-,1,3,1,-,4,1	0.943	2,-,4,1,3,1,-,-,1	0.964
40	2,-,-,1,3,1,1,4,-	0.844	2,-,-,1,3,1,-,4,1	0.898	2,-,4,1,3,1,1,-,-	0.934
48	3,-,-,-,2,1,1,4,1	0.756	2,-,-,1,3,1,-,4,1	0.816	2,-,4,1,3,1,-,-,1	0.874
56	3,-,-,-,2,1,1,4,1	0.769	2,-,-,1,3,1,-,4,1	0.825	2,-,4,1,3,1,-,-,1	0.879
64	3,-,-,-,2,1,1,4,1	0.722	3,-,-,1,2,1,-,4,1	0.776	2,-,4,1,3,1,-,-,1	0.831
72	3,-,-,-,2,1,1,4,1	0.654	3,-,-,1,2,1,-,4,1	0.712	3,-,4,1,2,1,1,-,-	0.776

Table 4
Optimal batteries distribution for different initial charge of the batteries and signal transmission ranges l_5, l_6.

	$l_5 = l_6 = 2$		$l_5 = l_6 = 3$		$l_5 = 5, l_6 = 4$	
Ω	b	$E(T)$	b	$E(T)$	b	$E(T)$
1.0	3,-,-,-,2,1,1,4,1	0.654	3,-,-,1,2,1,-,4,1	0.712	3,-,4,1,2,1,1,-,-	0.776
0.5	3,-,-,1,2,1,1,4,-	0.618	3,-,-,1,2,1,-,4,1	0.665	3,1,1,1,2,4,-,-,-	0.711
0.25	3,-,2,1,1,1,-,4,-	0.583	3,-,2,1,-,1,-,4,1	0.610	3,-,2,1,1,4,-,1,-	0.671
0.125	3,-,1,1,1,4,-,2,-	0.565	3,-,1,1,-,4,-,2,1	0.577	3,-,1,4,1,2,-,-,1	0.641
0	3,-,1,1,1,4,-,2,-	0.498	3,-,-,4,1,1,-,2,1	0.507	3,-,1,4,1,2,1,-,-	0.601

5.4. Influence of inter-maintenance time on ELC and optimal solutions

Fig. 11 presents the influence of the reduction of the inter-maintenance time T on the ELC $E(T)$ for different values of $l_5$and l_6 (for each combination of values of l_5, l_6 and T, the ELC is obtained for the optimal batteries distribution).

Table 3 presents the optimal batteries distribution for different system inter-maintenance times T and signal transmission ranges l_5, l_6. The non-monotonic behavior of $E(T)$ is explained by the fact that the fraction of the inter-maintenance time when the power sources are active and produce power can increase with increasing T. For example, the power sources are active for 13.3 h during 24 h (0.56% of time), whereas they are active for 21 h during 32 h (67% of time).

It can be seen that the inter-maintenance time T influences the optimal batteries distribution. For example, the first sensor should be equipped with a battery of type 2 when the time T is relatively short, but when the time increases, smaller but more reliable battery of type 3 becomes the better choice for the first node.

5.5. Influence of initial charge of the batteries on ELC and optimal solutions

Fig. 12 presents the influence of the reduction of initial charge of the batteries on the ELC $E(T)$ for different values of $l_5$and l_6 when $T = 72$. It is assumed that the initial charge of all the batteries is ωx_k (0), where x_k (0) is taken from Table 2. Table 4 presents the optimal batteries distribution for different initial charge of the batteries. It can be seen that the optimal batteries distribution depends on their initial charge. Intuitively, the ELC decreases when the initial charge of the batteries decreases.

6. Conclusions and further research topics

This paper pioneers the modeling and analysis of LCCSs with unreliable RGSs and storages, which work together to supply resource needed for each CE's operation, i.e., providing a certain connection range based on the specification. The following contributions have been made:

1) A numerical algorithm is proposed to evaluate the instantaneous availability of an individual CE with resource supply from the RGS and storage.
2) The effects of initial amount of resource and maximal downloading rate of the storage on the CE's instantaneous availability are investigated.
3) A universal generating function-based approach is implemented to evaluate the ILC for the considered LCCS with unreliable RGSs and storages.
4) The optimal storage allocation problem is formulated and solved, which determines the distribution of a limited number of storage units of different types to maximize the ELC.
5) Impacts of several model parameters on the ELC and the optimal storage allocation solutions are investigated through a detailed case study of a wireless sensor network with six batteries (storages) of four different types.

The case study demonstrates that the proposed optimization can improve the LCCS connectivity considerably, facilitating the optimal decisions on allocating limited storage units to LCCS nodes.

In this work, CEs, RGSs and storages are assumed to be non-repairable during the considered mission time. We plan to relax this assumption by considering the general repair model for the LCCS components. We are also interested in extending the model to consider phased mission operations, where the time-to-failure distributions of the LCCS components may vary from phase to phase due to dynamic environment conditions. Another direction of further research is to model the LCCS with multi-state CEs providing different connection ranges depending on resource supply rates.

CRediT authorship contribution statement

Gregory Levitin: Writing – original draft, Software, Methodology, Conceptualization. **Liudong Xing:** Writing – original draft, Formal analysis, Data curation. **Yuanshun Dai:** Supervision, Resources, Data curation.

Declaration of Competing Interest

There is no conflict of interests associated with this paper.

Data availability

No data was used for the research described in the article.

Acknowledgement

The work of L. Xing was partially supported by the National Science Foundation under Grant No. 2302094

References

[1] Zuo M, Liang M. Reliability of multistate consecutively-connected systems. Reliab Eng Syst Saf 1994;44:173–6.
[2] Gao K, Yan X, Peng R, Xing L. Economic design of a linear consecutively connected system considering cost and signal loss. IEEE Trans Syst Man Cybernet Syst 2021; 51(8):5116–28.
[3] Gao K, Peng R, Qu L, Xing L, Wang S, Wu D. Linear System Design with Application in Wireless Sensor Networks. J Indust Inform Integr 2022;27:100279. https://doi.org/10.1016/j.jii.2021.100279.
[4] Lei B, Ren Y, Wang Z, Ge X, Li X, Gao K. The Optimization of Working Time for a Consecutively Connected Production Line. Mathematics 2023;11(2):309. https://doi.org/10.3390/math11020309.
[5] Hwang F, Yao Y. Multistate consecutively-connected systems. IEEE Trans Reliab 1989;38:472–4.
[6] Levitin G. Universal generating function in reliability analysis and optimization. London: Springer-Verlag; 2005.
[7] Levitin G. Reliability evaluation for linear consecutively-connected systems with multistate elements and retransmission delays. Qual Reliab Eng Int 2001;17:373–8.
[8] Levitin G. Optimal allocation of multi-state elements in linear consecutively connected systems with vulnerable nodes. Eur J Oper Res 2003;150:406–19.
[9] Vasanthi T, Arulmozhi G. Optimal allocation problem using genetic algorithm. Int J Oper Res 2009;5(2):211–28.
[10] Levitin G, Xing L, Dai Y. Optimal allocation of connecting element in phase mission linear consecutively-connected systems. IEEE Trans Reliab 2013;62(3):618–27. https://doi.org/10.1109/TR.2013.2270413.

[11] Levitin G, Xing L, Dai Y. Connectivity Evaluation and Optimal Service Centers Allocation in Repairable Linear Consecutively Connected Systems. Reliab Eng Syst Safe 2018;176:187–93.
[12] Levitin G, Xing L, Dai Y. Linear multistate consecutively-connected systems subject to a constrained number of gaps. Reliab Eng Syst Safe 2015;133:246–52.
[13] Yu H., Yang J., Zhao Y. Reliability of phase mission linear consecutively-connected systems with constrained number of gaps. In: Safety and reliability of complex engineered systems: esrel 2015. CRC Press; pp. 1799–1803.
[14] Xiang Y, Levitin G, Dai Y. Linear multistate consecutively-connected systems with gap constraints. IEEE Trans Reliab 2012;61(1):208–14.
[15] Levitin G, Xing L, Ben-Haim H, Dai Y. m/nCCS: linear consecutively-connected systems subject to combined gap constraints. Int J Gen Syst 2015;44(7-8):833–48.
[16] Yu H, Yang J, Peng R, Zhao Y. Reliability evaluation of linear multi-state consecutively-connected systems constrained by m consecutive and n total gaps. Reliab Eng Syst Saf 2016;150:35–43.
[17] Levitin G, Xing L, Dai Y. Optimal arrangement of connecting elements in linear consecutively connected systems with heterogeneous warm standby groups. Reliab Eng Syst Safe 2017;165:395–401.
[18] Peng R, Xie M, Ng SH, Levitin G. Element maintenance and allocation for linear consecutively connected systems. IIE Trans 2012;44(11):964–73.
[19] Xing L, Levitin G. Connectivity modeling and optimization of linear consecutively connected systems with repairable connecting elements. Eur J Oper Res 2018;264(2):732–41.
[20] Cheng C, Yang J, Li L. Reliability assessment of multi-state phased mission systems with common bus performance sharing considering transmission loss and performance storage. Reliab Eng Syst Safe 2020;199:106917.
[21] Fink O, Zio E. Semi-Markov processes with semi-regenerative states for the availability analysis of chemical process plants with storage units. In: Proceedings of the Institution of Mechanical Engineers, Part O: Journal of Risk and Reliability. 227; 2013. p. 279–89.
[22] Hamada M, Martz HF, Berg EC, Koehler AJ. Optimizing the product-based availability of a buffered industrial process. Reliab Eng Syst Safe 2006;91(9):1039–48.
[23] Levitin G, Xing L, Dai Y. Optimal sequencing of elements activation in 1-out-of-n warm standby system with storage. Reliab Eng Syst Safe 2022;221:108380. https://doi.org/10.1016/j.ress.2022.108380.
[24] Qiu H, Yan X, Ma X, Peng R. Reliability of a phased-mission system with a storage component. Syst Sci Contr Eng 2018;6(1):279–92.
[25] Jia H, Peng R, Yang L, Wu T, Liu D, Li Y. Reliability evaluation of demand-based warm standby systems with capacity storage. Reliab Eng Syst Safe 2022;218(Part A):108132.
[26] Levitin G, Xing L, Dai Y. Optimal mission aborting in multistate systems with storage. Reliab Eng Syst Safe 2022;218(Part A):108086.
[27] Levitin G, Xing L, Dai Y. Unrepairable system with single production unit and n failure-prone identical parallel storage units. Reliab Eng Syst Safe 2022;222:108437.
[28] Levitin G, Xing L, Dai Y. Unrepairable system with consecutively used imperfect storage units. Reliab Eng Syst Safe 2022;225:108574.
[29] Curry RM, Smith JC. A survey of optimization algorithms for wireless sensor network lifetime maximization. Comp Indust Eng 2016;101:145–66.
[30] Levitin G, Xing L, Yu S. Optimal Connecting Elements Allocation in Linear Consecutively-Connected Systems with Phased Mission and Common Cause Failures. Reliab Eng Syst Safe 2014;130:85–94.
[31] Sharma H, Haque A, Jaffery ZA. Maximization of wireless sensor network lifetime using solar energy harvesting for smart agriculture monitoring. Ad Hoc Netw 2019;94:101966.
[32] Xing L. Reliability in Internet of Things: Current Status and Future Perspectives. IEEE Internet Things J 2020;7(8):6704–21. https://doi.org/10.1109/JIOT.2020.2993216.
[33] Xing L. Reliability Modeling of Wireless Sensor Networks: A Review. Recent Patent Eng 2021;15(1):3–11.
[34] Wang YD, Wu XH, Zhou ZL, Li YF. The reliability and lifetime distribution of SnO2- and CdSnO3-gas sensors for butane. Sens Actuat B Chem 2003;92(1–2):186–90. https://doi.org/10.1016/S0925-4005(03)00262-4.
[35] Le Z, Becker E, Konstantinides DG, Ding C, Makedon F. Modeling reliability for wireless sensor node coverage in assistive testbeds. In: Proceedings of the 3rd International Conference on Pervasive Technologies Related to Assistive Environments (PETRA '10). 46. New York, NY, USA: Association for Computing Machinery; 2010. p. 1–6. https://doi.org/10.1145/1839294.1839349.
[36] Kam OM, Noël S, Ramenah H, Kasser P, Tanougast C. Comparative Weibull distribution methods for reliable global solar irradiance assessment in France areas. Renew Energ 2021;165:194–210. https://doi.org/10.1016/j.renene.2020.10.151.
[37] Zhao Q, Jiang H, Chen B, Wang C, Xu S, Zhu J, Chang L. Research on State of Health for the Series Battery Module Based on the Weibull Distribution. J Electrochem Soc 2022;169(2). https://doi.org/10.1149/1945-7111/ac4f21.
[38] Levitin G. Genetic algorithms in reliability engineering. Guest Edit Reliab Eng Syst Safe 2006;91(9):975–6.
[39] Ildarabadi R, Lotfi H, Hajiabadi ME. Resilience enhancement of distribution grids based on the construction of Tie-lines using a novel genetic algorithm. Energ Syst 2023. https://doi.org/10.1007/s12667-022-00562-z.